

Revista Electrónica Nova Scientia

Phenomenological survey on the potential profile
evolution in III-V binary compounds

Panorama fenomenológico de la evolución del perfil
potencial de componentes binarios del grupo III-V

**Alejandro Mendoza Álvarez¹, Guillermo Fernández Anaya¹,
José Job Flores-Godoy¹, y Leo Diago-Cisneros^{1,2}**

¹ Depto. de Física y Matemáticas, Universidad Iberoamericana

² Facultad de Física, Universidad de La Habana, La Habana, Cuba

México - Cuba

Alejandro Mendoza, E-Mail: alejandro.mendoza@uia.mx

Resumen

En este artículo se analiza el cambio del perfil potencial dispersor en algunos compuestos, considerando el efecto de mezcla de huecos ligeros y pesados. Esto se obtiene aplicando el Teorema de Shur's Generalizado al problema cuadrático de autovalores obtenido a partir del problema que surge de un sistema de ecuaciones diferenciales N-acoplado del segundo orden, en el marco de la Aproximación de Masa Efectiva Multibanda. Consideramos energías incidentes menores, iguales y mayores que la altura de la barrera del potencial dispersor para diferentes compuesto binarios semiconductores del grupo III-V. En la descripción del perfil del potencial, empleamos el modelo de bandas de Kohn-luttinger (4x4) y (2x2) por completitud. Las propiedades estándar como pozo cuántico o barrera potencial de los compuestos binarios considerados, resultaron en lo general garantizadas, mas no todos los materiales seleccionados mostraron la evolución esperada en su perfil potencial: algunos que constituyen pozos cuánticos (QW) en aplicaciones tecnológicas, presentaron un comportamiento de barrera potencial efectiva (B) para huecos ligeros (lh), a diferentes rangos de energía incidente E y diferentes mezclas. En este estudio, ninguno de los compuestos con comportamiento de barrera en aplicaciones tecnológicas, evolucionó a un comportamiento de QW efectivo, válido tanto para lh como hh. Sorprendentemente todos los compuestos en este estudio que constituyen barreras en aplicaciones tecnológicas, presentaron transiciones desde QW a B para lh en el rango donde el valor de la energía es mayor que la altura de la barrera V_0 .

Palabras clave: Problema cuadrático de autovalores, perfil del potencial dispersor,

Recepción: 24-02-2011

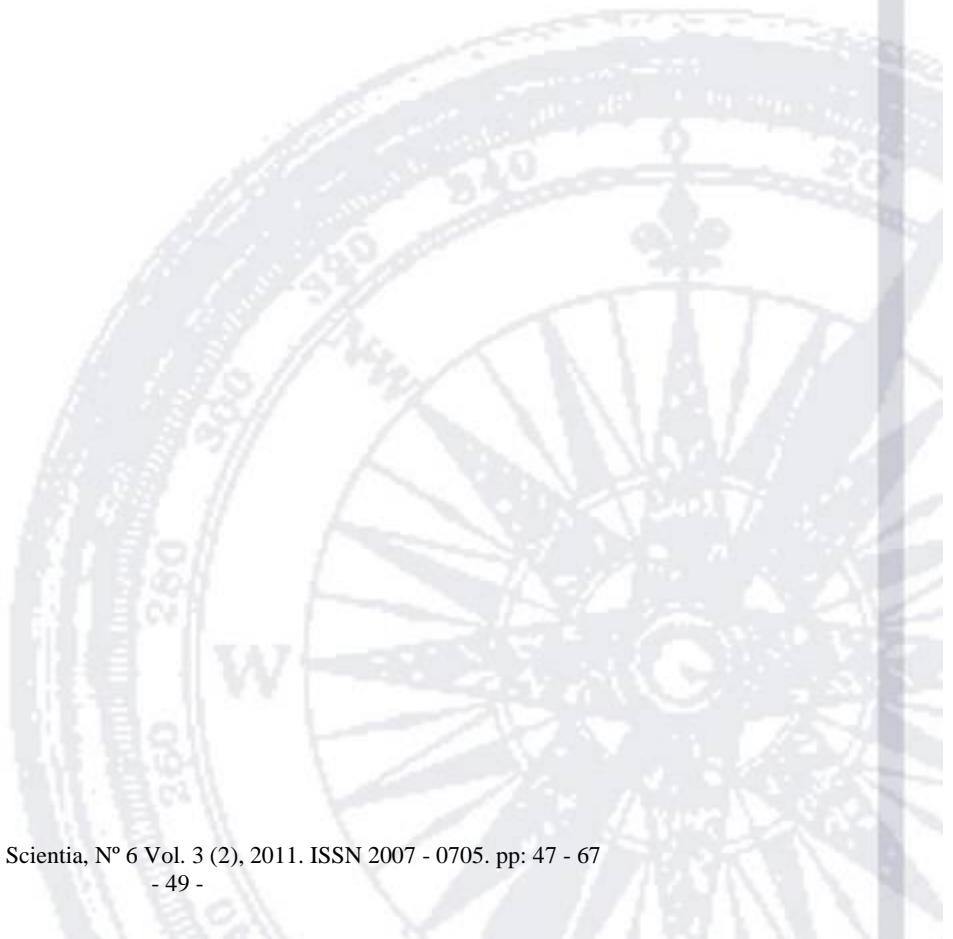
Aceptación: 11-04-2011

Abstract

In this paper we present the change in the effective potential profile of some compounds when the bandmixing of light and heavy holes is altered. We obtained this by applying Generalized Shur's Theorem to an eigenvalue quadratic problem obtained from a system with N second order coupled equations in the context of multiband effective mass approximation. We considered incident energy values that were lower, equal, and higher than the height of the dispersive

potential barrier for different III-V semiconductor binary compounds. Most of the standard properties of the binary compounds in this study were guaranteed; but not all of the materials we chose, have shown the evolution we expected in their effective potential profile: some of the ones that constitute quantum wells (*QW*) in technological applications only evolve into effective barrier (*B*) behaviors for light holes (*lh*) when they are in different incident energy (*E*) ranges and present different bandmixing. None of the barrier constituting compounds for technological applications in this study evolves into effective *QW* behaviors valid for both *lh* and *hh*. Surprisingly enough, all of the compounds in this study that constitute standard barriers in technological applications, present transitions from *QW* to *B* for *lh* in the range where the value of *E* is higher than the height of the barrier.

Key words: Quadratic eigenvalue problem, dispersing potential profile.



1 Outlines on non-linear eigenvalue problems

Quantum transport in multiband and multicomponent systems in the frame of envelope function approximation (EFA) [1] [2] might be efficiently dealt with through the analysis of a system with N second order coupled differential equations with a square eigenvalue and first derivative terms, also known as the quadratic eigenvalue problem (QEP). The QEP is currently receiving a lot of attention because it may be used in a wide variety of applications, and recently, in the study of quantum hole transport [3] [4]. In this model we prove that a base collected from the spinors of the QEP ($N \neq 1$) in a system of free particles does not fulfill classical orthonormalization [3], this uncommon scenario arises from terms that contain the first order derivative (that is responsible for the effects of the bandmixing of holes) that appear in the Kohn-Luttinger Hamiltonian. In spite of its obvious relevance, it is not considered by most authors. Usually, a generalized eigenvalue problem (GEP) is obtained from the QEP. Previous classical studies [5] may not be applied to the QEP-GEP problem since they prove that the corresponding matrices do not commute in the sense of Frobenius's theorem. More recent studies [6] [7] [8] [9] only provide the necessary conditions to solve GEP problems, and they do not work with the simultaneous triangularization of the corresponding matrices.

The dynamic equation -posed as a matrix invariant-boundary Sturm-Liouville problem under translations in the $[x; y]$ plane-, is given by [10] [11]:

$$\frac{d}{dz} \left[\mathbf{B}(z) \frac{d\mathbf{F}(z)}{dz} + \mathbf{P}(z)\mathbf{F}(z) \right] + \mathbf{Y}(z) \frac{d\mathbf{F}(z)}{dz} + \mathbf{W}(z)\mathbf{F}(z) = \mathbf{O}_{N \times 1}, \quad (1)$$

where $\mathbf{B}(z)$, $\mathbf{P}(z)$, $\mathbf{Y}(z)$ and $\mathbf{W}(z)$ are generally $(N \times N)$ Hermitian matrices, whose detailed form for concrete cases might be found in several published works [10] [11] [12]. From here onwards $\mathbf{O}_{N/N}$, will represent the null/identity matrix of a $(N \times 1)$ order. The N unknown functions are called envelope functions and they may be gathered under an N component vector that we shall call $\mathbf{F}(z)$, while z stands for the coordinate in the direction of quantization. The matrices fulfill the $\mathbf{B}(z)^\dagger = \mathbf{B}(z)$, $\mathbf{P}(z)^\dagger = \pm\mathbf{P}(z)$ and $\mathbf{W}(z)^\dagger = \mathbf{W}(z) = V(z) - E\mathbf{I}_N$ properties.

Therefore, by proposing the following solution to the differential problem Eq. (1):

$$\mathbf{F}(z) = \sum_{j=1}^{2N} \alpha_j e^{i\lambda_j z} \varphi_j = \sum_{j=1}^{2N} \alpha_j \mathbf{F}_j(z), \quad (2)$$

where α_j contains the quotients of the linear combination and the corresponding normalization constants of the $\mathbf{F}_j(z)$ in configuration space, λ_j is real or complex and φ_j is a $(N \times 1)$ spinor, we obtain the following algebraic problem that determines the QEP associated to Eq. (1)

$$\mathbf{Q}(\lambda)\varphi = \{\lambda^2 \mathbf{M} + \lambda \mathbf{C} + \mathbf{K}\} \varphi = \mathbf{O}_{N \times 1}, \quad (3)$$

where λ is the eigenvalue and the φ spinors are the eigenvectors (eigenspinors). Here, \mathbf{M} , \mathbf{C} and \mathbf{K} are $(N \times N)$ matrices, usually dependent on z . The general properties of the Eq. (3) might be found in Table 1 of reference [13]. We focused our attention on the case where \mathbf{M} , \mathbf{C} and \mathbf{K} are Hermitians, so λ is real or appears in (λ, λ^*) conjugated pairs, so it fits the systems that we are interested in, i.e. those described by Hamiltonians in the different cases of the $k \cdot p$ approximation [14]-[28].

A simple way to reach the linear form of Eq. (3) with identical eigenvalues is substituting $\mu = \lambda\varphi$ in Eq. (3), re-writing the equation as [13].

$$\{\lambda \mathbf{M} \mu + \mathbf{C} \mu + \mathbf{K} \varphi\} = \{\lambda \mathbf{M} + \mathbf{C}\} \mu + \mathbf{K} \varphi = \mathbf{O}_{N \times 1} \quad (4)$$

Which then leads us to the associated generalized eigenvalue problem (GEP) [1]

$$\begin{bmatrix} \mathbf{O}_N & \mathbf{N} \\ -\mathbf{K} & -\mathbf{C} \end{bmatrix} \begin{bmatrix} \varphi \\ \mu \end{bmatrix} - \lambda \begin{bmatrix} \mathbf{N} & \mathbf{O}_N \\ \mathbf{O}_N & \mathbf{M} \end{bmatrix} \begin{bmatrix} \varphi \\ \mu \end{bmatrix} = \{\mathbf{A} - \lambda \mathbf{B}\} \begin{bmatrix} \varphi \\ \mu \end{bmatrix} = \mathbf{O}_{2N \times 1}. \quad (5)$$

In general, we chose $N = I_N$ or one of the multiples of the identity matrix [13]. Other authors linearize the matrixial polynomial $\mathbf{Q}(\lambda)$ [29] in different ways; here $\mathbf{A} - \lambda \mathbf{B}$ is a $(2N \times 2N)$ matrix [13] [30].

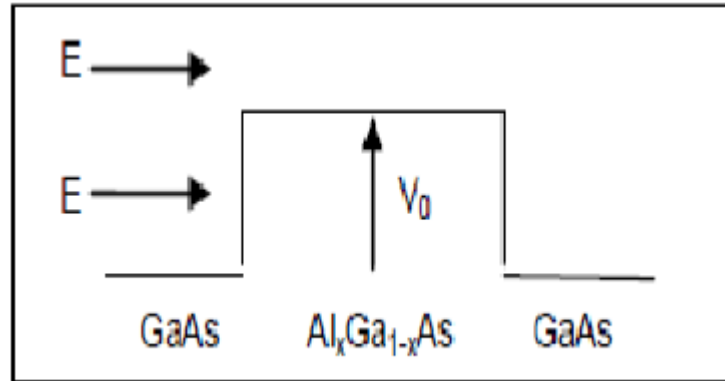


Figure 1: Incident energy values higher, equal, and lower than dispersion potential barrier height.

2 Basic background on potential profile changes with band- mixing

One of the most relevant problems for low-dimension heterostructured systems physics is the penetration of charge-carrier particles through potential barriers when their energy is lower than the height of the barrier. This is known as the charge-carrier quantum transport problem [31][32][33]. An extensive number of theoretical and experimental studies have been devoted to electrons [34][35], while there are just few studies that deal with quantum properties of stationary states in holes.

There have been some serious controversies among different research teams regarding light (lh) and heavy hole (hh) resonant tunneling [36][37]. A strong dependency of hole quantum transport physics upon the wave vector transversal to the main direction of transmission has been observed in the calculation of transport magnitudes (tunneling, transmission, diffusion, and so on). Early on, Wessel and Altarelli [38] proved the influence of hole bandmixing in resonant tunneling.

Several studies [39][40] have predicted the modification of the effective potential in the electronic case. Here the key lies in the fact that the behavior of both wells and effective barriers might appear in either of the materials of the binary alloy depending on the value of the transversal component of the wave vector [39].

All of the structures we study here are relevant for electronic and optoelectronic technological devices [41]. Here, we assume a rectangular distribution of potential energy (V_0) and a constant effective mass for each slab (see Fig. 1).

The theoretical frameworks described in the following section will allow us to undertake a detailed analysis of the evolution of the dispersion potential profile of III-V binary compounds, considering the hole bandmixing effect.

3 Numerical simulations and discussion

To obtain the physical observables associated to Eq.(5) we need to undertake a simultaneous diagonalization of matrices and through Shur's generalized decomposition [13] [42]. Two matrices, **A** and **B**, are simultaneously triangularizable when there is a similarity *U* transformation such that

$T_A = U^\dagger A U$ and $T_B = U^\dagger B U$ are superior triangular matrices.

As expected, the QEP associated to the M, C and K matrices in Eq. (3) has eight associated values with finite eigenvalues that are real or complex conjugated pairs:

$$\det(\kappa_z^2 \mathbf{M} + \kappa_z \mathbf{C} + \mathbf{K}) = 0. \quad (6)$$

The GEP's eigenvalues are calculated through a simultaneous triangularization of different binary compounds in the III-V group. As a workbench for our study we will use the widely known (4 × 4) Khon-Lüttinger's model (KL) in the shape [26]:

$$\mathbf{H}_{KL} = \begin{pmatrix} \mathbf{H}_{11} & \mathbf{H}_{12} & \mathbf{H}_{13} & 0 \\ \mathbf{H}_{12} & \mathbf{H}_{22} & 0 & -\mathbf{H}_{13} \\ \mathbf{H}_{13} & 0 & \mathbf{H}_{22} & \mathbf{H}_{12} \\ 0 & -\mathbf{H}_{13} & \mathbf{H}_{12} & \mathbf{H}_{11} \end{pmatrix}. \quad (7)$$

Where

$$\begin{aligned} \mathbf{H}_{11} &= A_1 \kappa_T^2 + V(z) - B_2 \partial^2 / \partial z^2, \\ \mathbf{H}_{12} &= (\hbar^2 \sqrt{3} / 2m_0) (\gamma_2 (\kappa_y^2 - \kappa_x^2) + 2i\gamma_3 \kappa_x \kappa_y), \\ \mathbf{H}_{13} &= (i\hbar^2 \sqrt{3} / 2m_0) \gamma_3 (\kappa_x - i\kappa_y) \partial / \partial z, \\ \mathbf{H}_{22} &= A_2 \kappa_T^2 + V(z) - B_1 \partial^2 / \partial z^2, \end{aligned}$$

With

$$\begin{aligned}
 A_1 &= \alpha_0^2 R (\gamma_1 + \gamma_2), & A_2 &= \alpha_0^2 R (\gamma_1 - \gamma_2), \\
 B_1 &= \alpha_0^2 R (\gamma_1 + 2\gamma_2), & B_2 &= \alpha_0^2 R (\gamma_1 - 2\gamma_2), \\
 \alpha_1 &= A_1 (\kappa_x^2 + \kappa_y^2) + V(z) - E, \\
 \alpha_2 &= A_2 (\kappa_x^2 + \kappa_y^2) + V(z) - E, \\
 h_{12} &= \alpha_0^2 R^2 \sqrt{3} \gamma_2 (\kappa_y^2 - \kappa_x^2),
 \end{aligned}$$

and γ_i , $i = 1, 2, 3$ [semi-empiric Luttinger parameters for valence band]; R [Rhydberg's constant]; α_0 [Bohr's radius]; $V(z)$ is the height of the stationary nite barrier; E [incident energy of propagation modes]; κ_x and κ_y [Components of the wave vector transversal to the direction of growth of the heterostructure (quasi-momentum components)].

The (4×4) KL's model describes the coupled shape of the bands in heavy and light holes of materials in groups IV, III-V, and II-VI, within the frame of the envelope function approximation (EFA) [1] [2]. It has $N = 4$ states that include the coupled form of holes (4 states: energy, momentum, angular momentum and spin-orbit interaction).

The binary compounds in the III-V alloy group have attracted the attention of "new" electronics (spintronics) [50], now that the era of the (crystaline and amorphous) Si has passed. The speed of the advance of semi-conductor technology has produced a promising interaction between theory and experimental knowledge. In the last few years, this knowledge has generated several kinds of low-dimensionality semi-conductor systems such as delta-doped systems, super networks, quantum wires, and quantum dots [44] [45] [46]. All of these systems have important applications in several fields, such as informatics, microelectronics, pharmaceutical and energy industries, as well as for environment protection.

Today, specialized scientific literature has not reported complete studies that specifically deal with the study of the evolution of the effective potential profile of binary compounds when there is a modification in the bandmixing of holes. This is why we consider that it is

important to undertake a wider study that involves incident energies values lower, equal, and higher than the dispersion potential barrier height.

In this work we did numeric simulations for several semi-conductor binary compounds (GaAs, GaP, GaN, InP, InAs, AlAs, AlP, AlN, AlSb) to obtain the evolution of the geometric place of the roots departing from the QEP with the (4x4) KL's model in the cases were: case 1 $E < V_0$, case 2 $E \sim V_0$ and case 3 $E > V_0$ (see Figs. 2, 3 and 4), considering the effect of the bandmixing of holes.

In the following figures we show the graphs for the real $\Re(\kappa_z)$ and imaginary $\Im(\kappa_z)$ parts of the geometric place of the κ_z roots of the QEP as a function of the κ_T hole bandmixing for $\kappa_x = \kappa_y$, $\kappa_x = \kappa_t$ and $\kappa_y = 0$, $\kappa_y = \kappa_T$ and $\kappa_x = 0$ directions and different incident energy values. The parameter is $\kappa_T = (\kappa^2 + \kappa^2)^{1/2}$

Most of hole state descriptions in literature are done through the (2x2) Kohn-Luttinger's model [47] based on orthonormalized linearly independent functions in the space of con guration.

Thus, by completion, and due to the symmetries that characterize the Hamiltonian Eq. (7), we have calculated the roots of Eq.(6) that correspond to the quadratic eigenvalue problem as a function of the bandmixing of holes using the (2x2) KL's model.

Diagonalizing the (4x4) KL's Hamiltonian [48]:

$$UH_{KL}U^\dagger = \Delta = \mathbf{I}_2 \otimes \lambda_{up}, \quad (8)$$

Where

$$U = \begin{pmatrix} \mathbf{u}_{up} & \mathbf{O}_2 \\ \mathbf{O}_2 & \mathbf{u}_{up} \end{pmatrix} U_e, \quad (9)$$

Being

$$U_e = \begin{pmatrix} \mathbf{I}_2 & \mathbf{O}_2 \\ \mathbf{O}_2 & \sigma_x \end{pmatrix} U_b. \quad (10)$$

Broido and Sham's matrix [49] U_b , is given as

$$U_b = \begin{pmatrix} e^{-i\Phi} & 0 & 0 & -e^{-i\Phi} \\ 0 & e^{-i\eta} & -e^{-i\eta} & 0 \\ 0 & e^{i\eta} & e^{i\eta} & 0 \\ e^{i\Phi} & 0 & 0 & e^{i\Phi} \end{pmatrix}, \quad (11)$$

where

$$\eta = \frac{1}{2} \left\{ \arctan \left(\frac{\kappa_x}{\kappa_y} \right) - \arctan \left(\frac{2\gamma_3 \kappa_x \kappa_y}{\gamma_2 (\kappa_y^2 - \kappa_x^2)} \right) \right\}, \quad (12)$$

and

$$\Phi = \frac{1}{2} \left\{ \arctan \left(\frac{\kappa_x}{\kappa_y} \right) + \arctan \left(\frac{2\gamma_3 \kappa_x \kappa_y}{\gamma_2 (\kappa_y^2 - \kappa_x^2)} \right) \right\}. \quad (13)$$

The matrix U_b carries out the transformation

$$U_b \mathbf{H}_{KL} U_b^\dagger = \begin{pmatrix} \mathbf{H}_{up} & \mathbf{O}_2 \\ \mathbf{O}_2 & \mathbf{H}_{low} \end{pmatrix}, \quad (14)$$

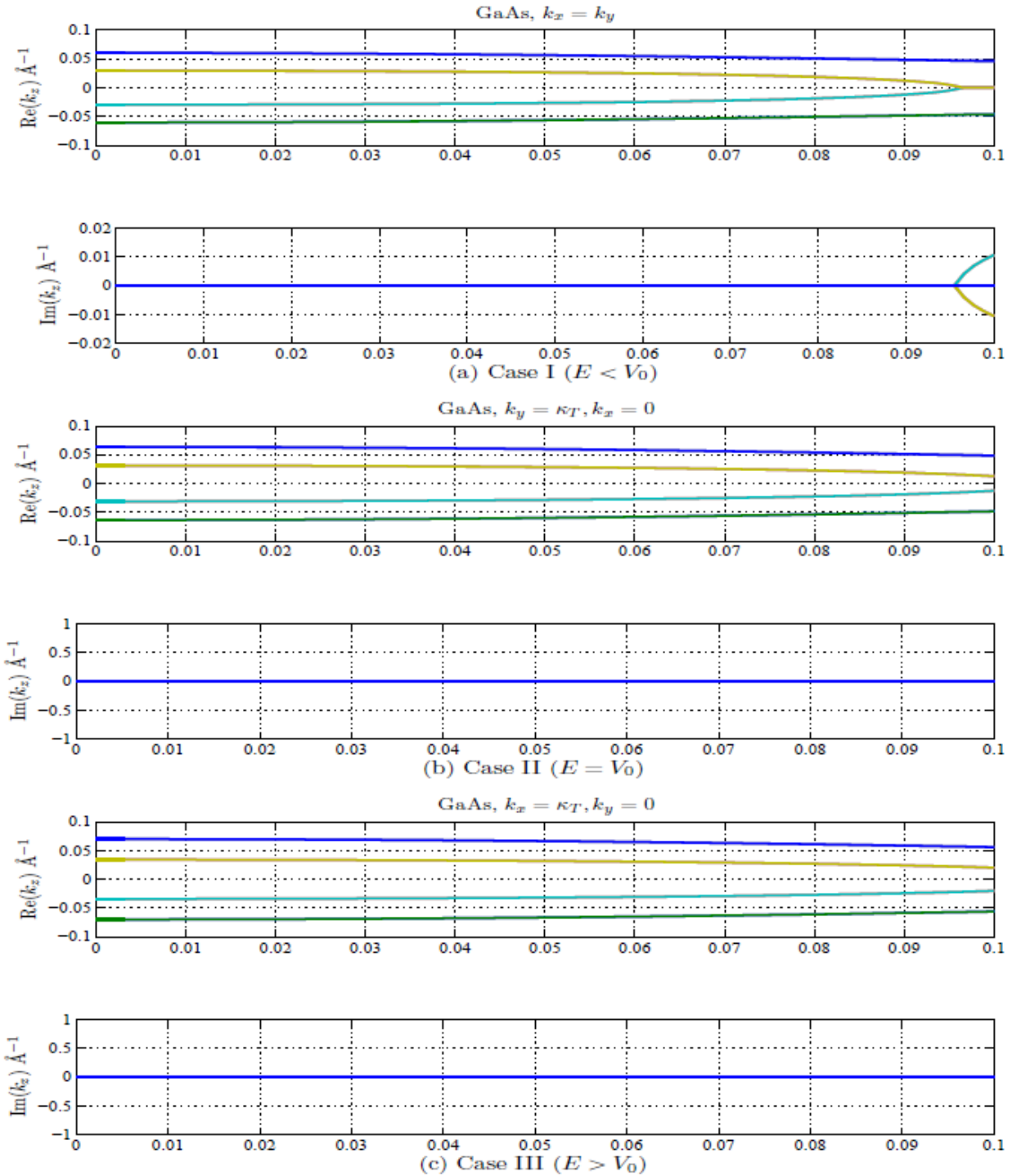


Figure 2: Geometric map of the κ_z eigenvalues of the QEP for the GaAs as a function of κ_T for different incident energy values. We assume that $V(z) = 0$ and we use the (4×4) KL's model. The external tracts belong to heavy holes (hh), while those inside correspond to light holes (lh). In a) we show the case where $E < V_0$ with $E =$

0.45eV in the [11] direction for the real and imaginary part respectively as a function of the bandmixing of holes. Eigenvalues are real for (*lh*) in the [0, 0.96] interval, while they are imaginary for (*l \bar{h}*) in the [0.96, 1] interval; eigenvalues are real for (*hh*) for every hole bandmixing value. In turn, b) and c) belong to the case when $E \sim V_0$ with $E = 0.498eV$ and when $E > V_0$ with $E = 0.60eV$ in the [01] and [10] directions respectively. In the plane transversal to the inner faces, eigenvalues are real for both (*lh*) and (*hh*) for every bandmixing value.

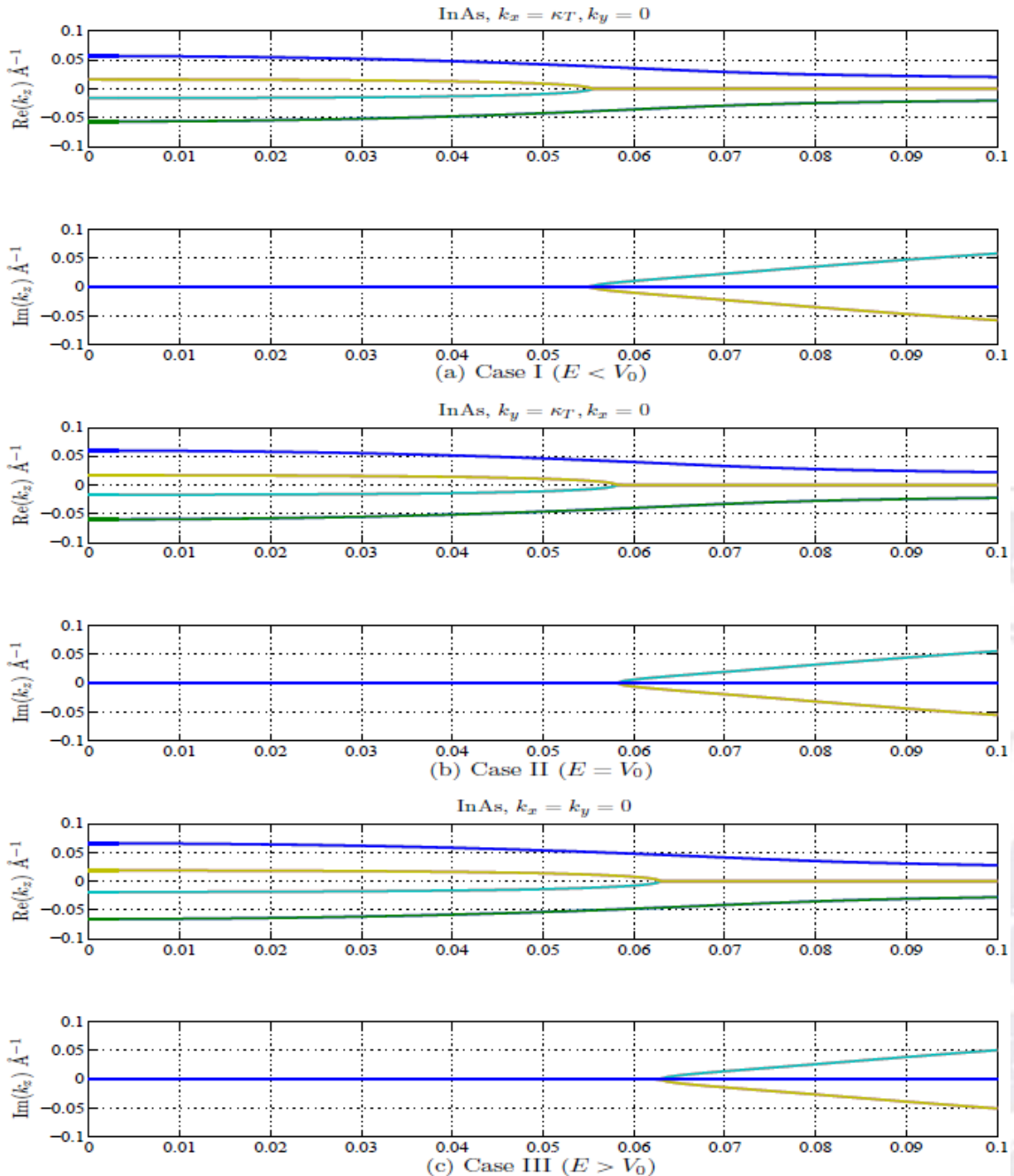
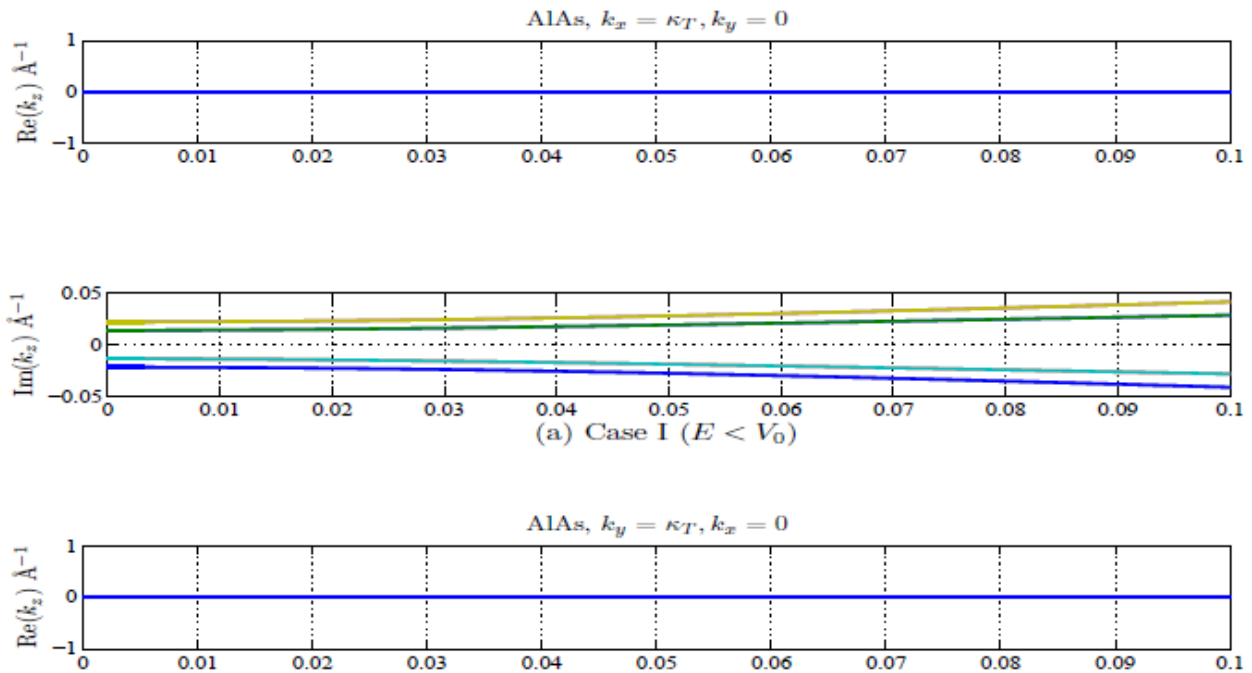


Figure 3: Geometric map of the κ_z eigenvalues of the QEP for InAs as a function of κ_T for different values of incident energy. We assume that $V(z) = 0$ and we use the (4×4) KL's model. External tracts belong to heavy holes (hh), while the inner ones correspond to light holes (lh). In a) we show the case where $E < V_0$ with $E = 0.45eV$ in the [10] direction for the real and imaginary parts respectively, as a function of hole bandmixing. Eigenvalues are real for (lh) in the $[0, 0.55]$ interval, and they are imaginary for (lh) in the $[0.55, 1]$ interval, eigenvalues are real for (hh) in all the bandmixing. In b) we show the case where $E \sim V_0$ with $E = 0.498eV$ in the [01] direction, eigenvalues are real for (lh) in the $[0, 0.58]$ interval; and imaginary for (lh) in the $[0.58, 1]$ interval, while eigenvalues are real for (hh) in all the bandmixing. In c) we show $E > V_0$ with $E = 0.60eV$ in the [11] direction, there, eigenvalues are real for (lh) in the $[0, 0.62]$ interval; imaginary for (lh) in the $[0.62, 1]$ interval, and eigenvalues are real for (hh) in all the bandmixing.



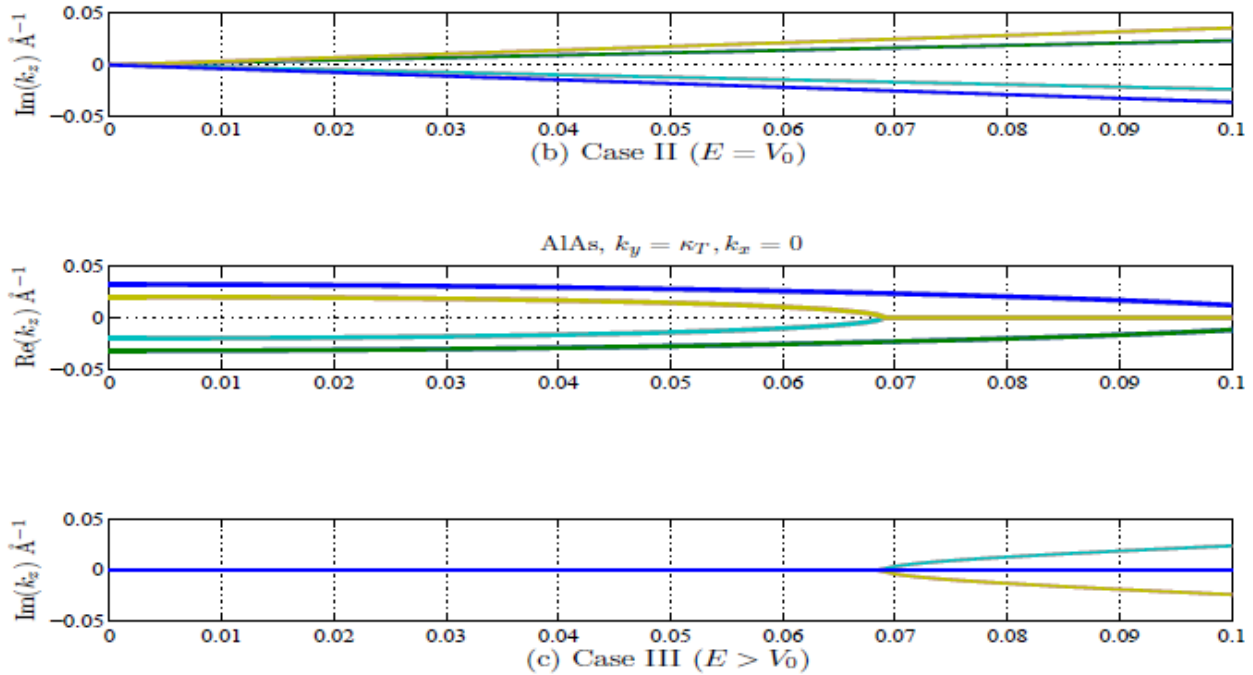


Figure 4: Geometric map of the κ_z eigenvalues for the QEP for AlAs as a function of κ_T at different incident energy values. We assume that $V(z) = 0.498\text{eV}$ and use the (4×4) KL's model. External tracts belong to heavy holes (hh), while inner tracts belong to light holes (lh). In a) we show the case when $E < V_0$ with $E = 0.45\text{eV}$ in the direction [01] for the real and imaginary parts respectively as a function of the bandmixing of holes, the eigenvalues are imaginary for (lh) and for (hh) in all the bandmixing, as in the case of $E \sim V_0$ with $E = 0.498\text{eV}$, which is shown in b) for the direction [01]. The case shown in c) corresponds to an $E > V_0$ with $E = 0.60\text{eV}$ in the direction [11], the eigenvalues are real for (lh) in the $[0, 0.69]$ interval, while they are imaginary for (lh) in the $[0.69, 1]$ interval, eigenvalues are real for (hh) in all the bandmixing.

SO

$$\left\{ \begin{array}{l} \mathbf{u}_{up} \mathbf{H}_{up} \mathbf{u}_{up}^\dagger = \lambda_{up} \\ \mathbf{u}_{low} \mathbf{H}_{low} \mathbf{u}_{low}^\dagger = \lambda_{low} \end{array} \right\}. \quad (15)$$

λ_{up} y λ_{low} are (2×2) diagonal matrices containing the eigenvalues

$$\mathbf{H}_u = \begin{bmatrix} A_1\kappa_T^2 + B_2\kappa_z^2 + V(z) & C_{xy} - iD_{xy}\kappa_z \\ C_{xy} + iD_{xy}\kappa_z & A_2\kappa_T^2 + B_1\kappa_z^2 + V(z) \end{bmatrix}, \quad (16)$$

$$\mathbf{H}_l = \begin{bmatrix} A_2\kappa_T^2 + B_1\kappa_z^2 + V(z) & C_{xy} - iD_{xy}\kappa_z \\ C_{xy} + iD_{xy}\kappa_z & A_1\kappa_T^2 + B_2\kappa_z^2 + V(z) \end{bmatrix}, \quad (17)$$

where the Hamiltonians \mathbf{H}_u and \mathbf{H}_l correspond to the sub-spaces up (u) and low (l), both with a (2×2) dimension.

Fig.5 shows the graphs for the real $\Re(\kappa_z)$ and imaginary $\Im(\kappa_z)$ parts of the geometric place of the roots κ_z of the QEP for the cases where $E < V_0$, $E \sim V_0$, and $E > V_0$, considering the effect of the bandmixing of holes, using the \mathbf{H}_u and \mathbf{H}_l Hamiltonians. Although not shown here the (2×2) KL's model owing to brevity, we have observed no differences between the cases where $E < V_0$ and $E \sim V_0$ in comparison to the results obtained from the (4×4) KL's model Hamiltonian, which guaranteed its standard barrier properties. Nevertheless, in the case where $E > V_0$, both the heavy (hh) and the light holes (lh) presented a quantum well (QW) in the $[0.0, 13]$ interval because their eigenvalues were real; while heavy (hh) and light holes (lh) simultaneously experienced an attractive and repelling energy in the $[0.13, 0.49]$ interval, since their eigenvalues were complex- real part and imaginary part. In the $[0.49, 0.64]$ interval, both light (lh) and the heavy holes (hh) experienced a barrier; finally in the $[0.64, 1]$ interval light holes (lh) experienced a quantum well, while heavy holes (hh) presented a barrier. The results were the same independently of the use of \mathbf{H}_u or \mathbf{H}_l Hamiltonians respectively.

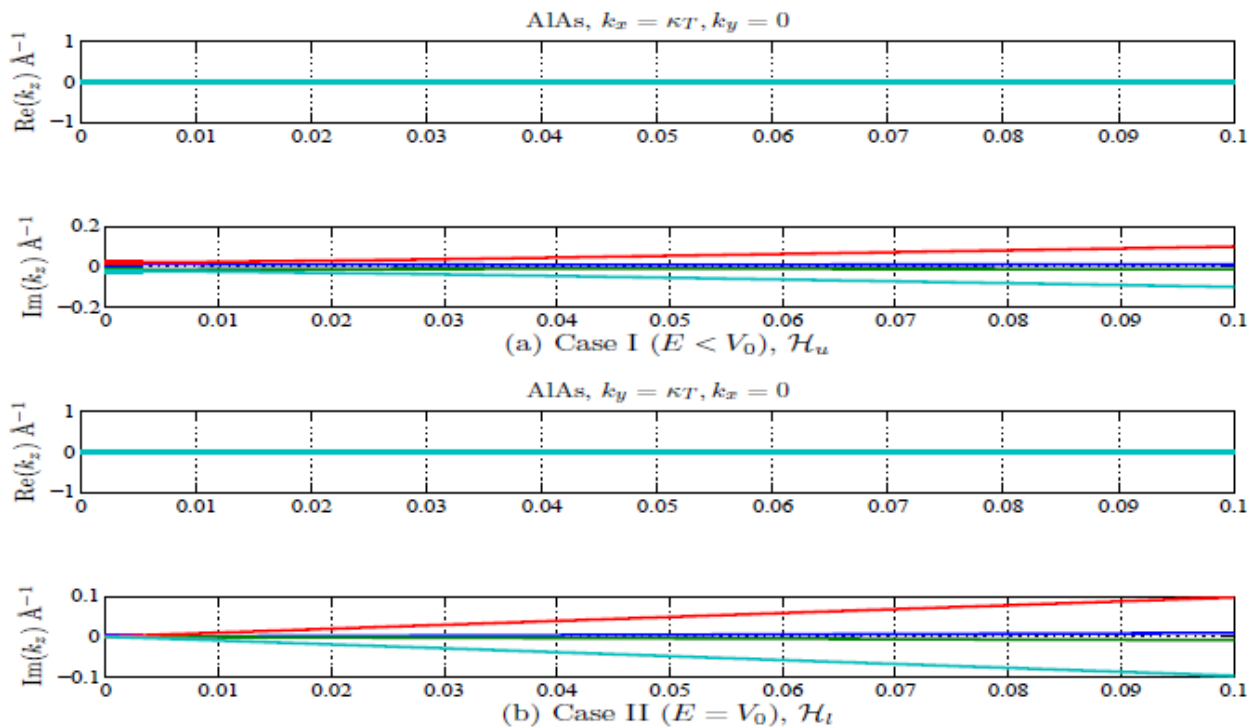
The study of AlP, AlN and AlSb binary semiconductors using the (2×2) Kohn-Luttinger's band models resulted in a behavior similar to the one observed for the AlAs highlighted in Fig. 5. Several of the typical (recurrent) features in Table 1 are worthy of consideration, since not all of the potential profiles of the materials in this study show the expected evolution. Some of the compounds in this study that constitute quantum wells (QW) in technological applications for massive particles and quasi-particles some only presented an effective barrier behavior (B) for light holes (lh) with different bandmixing and ranges

of incident energy (E).

In the case of the InAs (see Fig. 3) we find that heavy holes (hh) experience a well independently of incident energy and the value of the bandmixing, just as the light holes (lh) until the bandmixing reaches a critical value of $\kappa T = 0.62$, and from then on they display barrier behavior.

The standard properties of GaP, GaN and InP binary semi-conductor compounds as potential wells are guaranteed for both heavy (hh) and light holes (lh), independently of incident energy and bandmixing values.

Both heavy (hh) and light holes (lh) in AlAs experience a barrier in the cases where incident energy values are lower or equal to dispersion potential barrier height, since the eigenvalues are purely imaginary. Nevertheless, in the case where $E > V_0$, heavy holes (hh) experience a well independently of the bandmixing value, and light holes (lh) also present a well when the bandmixing is low and the barrier reaches a critical value of $\kappa T = 0.69$. In the [01], [10] and [11] directions respectively there are no changes in behavior.



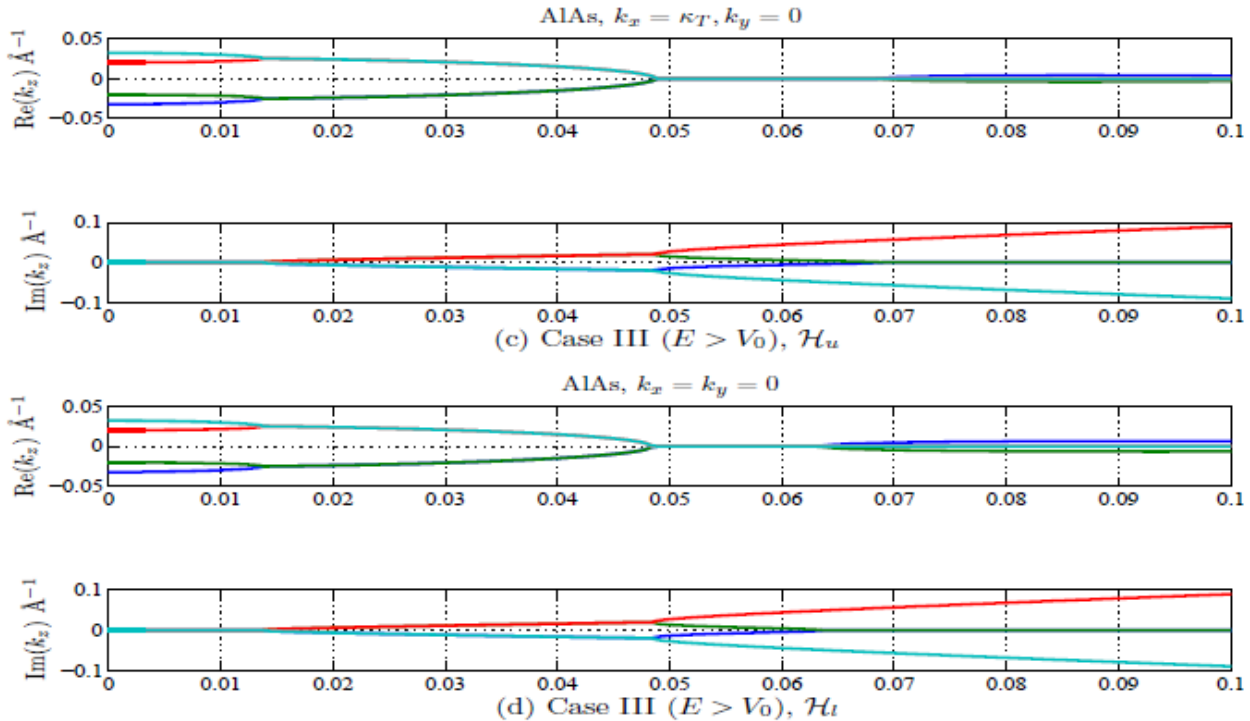


Figure 5: Geometric map of the κ_z eigenvalues of the QEP for AIAs as a function of κ_T at different values of incident energy. We assume that $V(z) = 0.498eV$ and use H_u and H_l respectively. External tracts correspond to heavy holes (hh) while inner ones belong to light holes (lh). In a) we show the case where $E < V_0$ with $E = 0.45eV$ in the direction $[10]$ using the H_u Hamiltonian; the eigenvalues for both (lh) and (hh) are imaginary for all the bandmixing, just as in the case where $E \sim V_0$ with $E = 0.498eV$ in figure b) for direction $[01]$, using the H_l Hamiltonian. In c) we show the case where $E > V_0$ with $E = 0.60eV$ in the $(1, 0)$ direction, using the H_u Hamiltonian, eigenvalues are real in the $[0, 0.13]$ interval, and complex for (lh) and (hh) in the $[0.13, 0.48]$ interval, eigenvalues are imaginary for (lh) and (hh) in the $[0.48, 0.68]$ interval, real for (lh) in the $[0.68, 1]$ interval and imaginary for (lh) in the $[0.68, 1]$ interval. In d) we show the case where $E > V_0$ with $E = 0.60eV$ in the direction $[11]$, using the H_l Hamiltonian, the eigenvalues are real for (lh) and (hh) in the $[0, 0.13]$ interval, complex for (lh) and (hh) in the $[0.13, 0.49]$ interval, imaginary for (lh) and (hh) in the $[0.49, 0.64]$ interval. Finally, eigenvalues are real for (lh) in the $[0.64, 1]$ interval and imaginary for (hh) in the $[0.64, 1]$ interval.

Compound/ Charge Carrier	Case I (<i>lh</i>)	Case I (<i>hh</i>)	Case II (<i>lh</i>)	Case II (<i>hh</i>)	Case III (<i>lh</i>)	Case III (<i>hh</i>)
GaAs	$QW \rightarrow B$	QW	QW	QW	QW	QW
GaP	QW	QW	QW	QW	QW	QW
GaN	QW	QW	QW	QW	QW	QW
InP	QW	QW	QW	QW	QW	QW
InAs	$QW \rightarrow B$	QW	$QW \rightarrow B$	QW	$QW \rightarrow B$	QW
AlAs	B	B	B	B	$QW \rightarrow B$	QW
AIP	B	B	B	B	$QW \rightarrow B$	QW
AlN	B	B	B	B	$QW \rightarrow B$	QW
AlSb	B	B	B	B	QW	QW

Table 1: Evolution in the potential profile of different binary semi-conductor compounds of the III-V groups when incident energy values are lower, equal, and higher than the dispersion potential barrier height with different hole bandmixing values. For the GaAs (see Fig. 2), and independently of incident energy and the value of the bandmixing, we find that all the eigenvalues are real for the heavy holes (*hh*). Therefore, the envelope function (2) is oscillatory in this case, and those holes experience a quantum well (QW); the light holes (*lh*) also experience a well when incident energy values are equal or higher than the dispersion potential barrier height; but not in the case where $E < V_0$, where the eigenvalues are purely imaginary once that the bandmixing has reached the critical value $\kappa T = 0.96$, so the envelope function (2) is not oscillatory and, therefore holes present barrier behavior.

We observed that the behavior of AIP, AlN and AlSb is identical to the one obtained for the AlAs in the cases where incident energy values are lower, equal and higher than dispersion potential barrier height in the different directions.

4 Final remarks

The standard properties of AlAs, AIP, AlN, and AlSb binary compounds, with a typical barrier behavior [41] where guaranteed through the use of the (4×4) Kohn-Luttinger's band model for any value of the bandmixing in the cases where incident energy values were lower or equal to the height of the dispersion potential barrier. Nevertheless, and according to Milanovic's predictions [39] *hh* experienced an effective QW independently of the bandmixing value, whereas *lh* experienced an effective QW when bandmixing values were low and a barrier when the bandmixing reached a critical value. Thus, for *lh* in all

of the barrier constituting compounds in the present study (used in technological applications) we found transitions from a QW to an effective B type behavior when the incident energy values were higher than the barrier height. The lh and hh in all of the GaP, GaN, and InP binary semi-conductor compounds with a typical QW behavior [41] experienced an effective QW for every incident energy value, independently of the bandmixing; whereas the lh in GaAs and InAs compounds experienced a barrier, when the bandmixing reached a critical value. In general, no differences were observed when using the (2×2) Kohn-Luttinger's band model for energy values lower or equal to dispersion potential barrier height in relation to the results obtained when using the (4×4) Kohn-Luttinger's model; nevertheless this behavior changes when the energy values are higher than dispersion potential barrier height. It is a straightforward observation that lh are heavier than hh for strong bandmixing and increasing incident energy; i.e., whenever the branches of lh are the widest open ones. Therefore we reinforce the widely known assertion according to what the hole labelling in light and heavy quasi-particles is only adequate for low values of the energy and bandmixing. This does not only allow for a better understanding of effective potential profile evolution in binary compounds when the hole bandmixing is modified [41] [39] [40] but is also allows us to think of potential applications in the design of quantum "lithers" that are so relevant in electronic and optoelectronic device design and development.

References

- [1] M. G. Burt, J. Phys. Condens. Matter 4, 964 (1992).
- [2] B. A. Foreman, Phys. Rev. B 48, 4964 (1993).
- [3] L. Diago-Cisneros, H. Rodríguez-Coppola, R. Pérez-Álvarez, and P. Pereyra, Phys. Rev. B 74, 045308 (2006).
- [4] L. Diago-Cisneros, G. Fernández-Anaya and G. Bonfanti-Escalera, Phys. Scr. 78, 035004 (2008).
- [5] Neal H. McCoy, Bull. Amer. Math. Soc., 42:592, 600 (1936).
- [6] C. B. Moler and G. W. Stewart, SIAM J. Numer. Anal. 10, 241 (1973).
- [7] M. Haardt, K. Häuper, J. Moore and J. Nossek, Proceedings of EUSIPCO-96", (Trieste, Italy, 1996) vol.1, pp.531- 534.
- [8] M. Haard and J. A. Nossek, IEEE 46, 161 (1998).
- [9] L. de Lathauwer, B. de Moore, and J. Vandewalle, SIAM J. Matrix Anal. Appl. 26, 295 (2004).

- [10] A. M. Malik, M. J. Godfrey and P. Dawson, *Phys. Rev. B* 59, 2861 (1999).
- [11] R. Pérez-Álvarez, C. Trallero-Herrero and F. García-Moliner, *European Journal of Physics* 22, 275 (2001).
- [12] L. Diago-Cisneros, H. Rodríguez-Coppola, R. Pérez-Álvarez, P. Pereyra, arXiv:cond- mat/0410159v1, 6 Oct (2004).
- [13] F. Tisseur and K. Meerbergen, *SIAM Review* 43, 235 (2001).
- [14] D. A. Broido and L. J. Sham, *Phys. Rev. B* 31, 888 (1985).
- [15] L. C. Andreani, A. Pasquarello and F. Bassani, *Phys. Rev. B* 36, 5887 (1987).
- [16] E. P. O'Reilly and G. P. Witchlow, *Phys. Rev. B* 34, 6030 (1986).
- [17] G. Schechter, L. D. Shvartsman and J.E. Golub, *J. Appl. Phys.* 78, 288 (1995).
- [18] S. S. Nedorezov, *Fiz. Tverd. Tela* 12, 2269 (1970) [*Sov. Phys. Solid State* 12, 1814 (1971)].
- [19] J. N. Schulman and Yia-Chung Chang, *Phys. Rev. B* 31, 2056 (1985).
- [20] Yia-Chung Chang and J. N. Schulman, *Phys. Rev. B* 31, 2069 (1985).
- [21] U. Ekenberg, L. C. Andreani and A. Pasquarello, *Phys. Rev. B* 46, 2625 (1992).
- [22] Z. Ikonc and V. Milanovic, *Phys. Rev. B* 45, 8760 (1992).
- [23] Z. Ikonc, V. Milanovic and D. Tjapkin, *Phys. Rev. B* 46, 4285 (1992).
- [24] A. D. Sánchez and C. R. Proetto, *J. Phys. Condens. Matter* 7, 2059 (1995).
- [25] G. Goldoni and A. Fasolino, *Phys. Rev. B* 51, 9903 (1995).
- [26] L. Diago-Cisneros, H. Rodríguez-Coppola and R. Pérez-Álvarez, *Rev. Mex. Fis.* 46, 337 (2000).
- [27] G. Goldoni and A. Fasolino, *Phys. Rev. Lett.* 69, 2567 (1992).
- [28] G. Goldoni and A. Fasolino, *Surf. Sci.* 305, 333 (1994).
- [29] P. Lancaster, "Lambda-Matrices and Vibrating Systems" (Editorial Pergamon Press, Oxford, UK), 1966.
- [30] I. Gohberg, P. Lancaster y L. Rodman, "Matrix Polynomials" (Editorial Academic Press, New York), 1982.
- [31] R. Tsu and L. Esaki, *Appl. Phys. Lett.* 22, 562 (1973)
- [32] P.A. Mello, P. Pereyra, and N. Kumar, *Ann. Phys.* 181, 290 (1988)
- [33] P. Pereyra, *Phys. Rev. Lett.* 80, 2677 (1998)
- [34] M. C. Payne, *J. Phys. C* 19, 1145 (1986)
- [35] P. Weetman and M.S. Wartaka, *J. Appl. Phys.* 93, 9562 (2003)
- [36] M. Nido, M.G. Alexander, W.W. Rühle, and K. Köhler, *Phys. Rev. B* 43, 1839 (1991).
- [37] L. Kadanof et al., *Phys. Rev. B* 42, 7065 (1990)
- [38] R. Wessel and M. Altarelli, *Phys. Rev. B* 39, 12802 (1989).
- [39] V. Milanovic, and D. Tjapkin, *Phys. Stat. Sol(b)* 110, 685 (1988).
- [40] Rolando Pérez-Álvarez and Federico García-Moliner, *Transfer Matrix, Green Function and related techniques: Tools for the study of multilayer heterostructures*, (ed. Universitat Jaume I, Castellón de la Plana, España), 2004.
- [41] I. Vurga man, J. R. Mayer, and L. R. Ram-Moham, *J. App. Phys* 89:11, 5815 (2001).
- [42] G.H. Golub and C.F. van Loau, *Matrix Computations*, Oojns Hopkins University Press, 3rd. ed. Baltimore, USA (1996).
- [43] David D. Awschalom and M. Flatt e, *Nature* 3, 153 (2007)
- [44] L. Esaki, *J. Physique* 45, C5 (1984).
- [45] R. Pérez- Álvarez, *Propiedades de heteroestructuras semiconductoras cuánticas*, Vol 1, pp. 41 (Revista: 100cias@uned, UNED, Madrid, 1984).

- [46] H. Sakaki, Solid State Communications 92, 119 (1994).
- [47] J. M. Luttinger and W Kohn, Phys. Rev. 97:4, 869-883 (1955).
- [48] L. Diago-Cisneros, H. Rodriguez-Coppola, R. Pérez Álvarez, and P. Pereyra, Phys. Scripta 71, 582 (2005)
- [49] D. A. Broido and L.J. Sham, Phys. Rev. B 58, 165 (1985)
- [50] H. Shapiro, Pacific Journal of Mathematics 181:3, 323 (1997).

